



Voltage control loss factors for quantifying DG reactive power control impacts on losses and curtailment

Matthew Deakin¹  | Thomas Morstyn² | Dimitra Apostolopoulou³  | Malcolm D McCulloch⁴

¹ School of Engineering, Newcastle University, Newcastle-upon-Tyne, UK

² School of Engineering, University of Edinburgh, Edinburgh, UK

³ Department of Electrical and Electronic Engineering, City, University of London, London, UK

⁴ Department of Engineering Science, University of Oxford, Oxford, UK

Correspondence

Matthew Deakin, School of Engineering, Newcastle University, Newcastle-upon-Tyne, UK.
Email: matthew.deakin@newcastle.ac.uk

Funding information

Newcastle University; Oxford Martin Programme on Integrating Renewable Energy; Clarendon Scholarship

Abstract

Distributed Generators that use reactive power for voltage control in distribution networks reduce renewable curtailment but can significantly increase network losses, undermining the effectiveness of this control. This paper proposes Voltage Control Loss Factors (VCLFs) as a means of understanding the interactions between reactive power flows, losses and curtailment, focusing on commercial-scale generators in radial systems. The metric uses a substitution-based method, whereby a system with voltage control is compared against a counterfactual with no such control. The proposed method studies this metric by coupling numerically precise black-box simulations with analytic results from a Two-Bus network representation. The latter provides a physical explanation for the numerical simulation results in terms of power, voltage and impedance parameters, providing clear explainability which is absent in traditional approaches for determining distribution loss factors. The whole solution space of the Two-Bus system is explored, and VCLFs are calculated for six cases on three unbalanced test networks to illustrate the approach. Relative losses as high as 30% are found in a system with high branch resistance-reactance ratio and large voltage rise. The results have implications for the design of loss allocation algorithms in distribution networks, and the optimal sizing of power-electronic interfaced Distributed Generators.

1 | INTRODUCTION

This paper proposes a metric for quantifying impacts that voltage control can have on relative losses when distributed generators (DGs) use reactive power for reducing curtailment, and combines both analytic and simulation-based approaches to study how this metric varies across network construction types and voltage levels. Drawing reactive power from DGs ameliorates voltage rise caused by real power injections, but this usually increases line currents and therefore also losses [1], thereby diminishing the benefits of the voltage control scheme. Failing to account for these additional losses due to voltage control potentially leads to market distortions in liberalised energy systems, leading to inefficient outcomes. For example, site-specific Distribution Loss Factors [2] (or 'Line Loss Factors') are not calculated in the GB system below 33 kV [3], and

so generators at these voltage levels are incentivised to reduce curtailment irrespective of changes in network operational costs.

There are many works that consider the interplay between DG curtailment and losses numerically via simulations. In [4], losses increase by up to 28% when voltage control from generators is taken into account in an active network management scheme, whilst [5] estimates marginal loss factors of 2.5% that can be ascribed to DGs. In [6], the authors design volt-var curves for LV networks, with the result that losses more than double in some cases. The work of [7] develops a scheme for loss minimization and voltage control of wind farms on an HV distribution system, although in this case relative losses are reduced by no more than 4%, showing relatively modest benefits from that control. Other works study optimal curtailment and scheduling of DGs to minimise losses [8, 9].

This is an open access article under the terms of the [Creative Commons Attribution](https://creativecommons.org/licenses/by/4.0/) License, which permits use, distribution and reproduction in any medium, provided the original work is properly cited.

© 2022 The Authors. *IET Generation, Transmission & Distribution* published by John Wiley & Sons Ltd on behalf of The Institution of Engineering and Technology

In general, however, without coupling numerical simulations with a suitable analytic approach, it is challenging to assess the generality of the results in systems with varying levels of demand or branch resistance-reactance ratio (R/X) ratio [10]. It is also worth noting that Distribution Loss Factors used in loss allocation [2] are usually determined using simulation-based approaches, with loss factors calculated via either explicit or implicit calculations of expected losses caused by a consumer.

In contrast, by combining a chosen simulation approach with a simplified, parameterised model, general conclusions can be drawn about systems which share the essential characteristics of that model. In [10], the authors compare the relative performance of volt-var control schemes for a range of LV network configurations, demonstrating the key role that control settings play in the interaction between curtailment and losses. The previous work by the authors briefly considers the error in an estimation of the valuation of reactive power control, should losses be ignored, as a function of R/X ratio [11]. In [12], it is noted that losses due to DGs follow a ‘U-shape’ curve with respect to DG penetration: losses first decline as the penetration of DG increases, before starting to increase. Other analytic approaches for understanding distribution systems behaviour include [13], which demonstrates there is only a weak link between R/X ratio, load power factor and voltage when compared to the line length; and [14], which considers how maximum power transfer is affected as a function of impedance angle. The importance of using these sorts of analytic approaches is stressed by the Cigré working group on Planning and Optimization of Active Distribution Systems, who note that ‘...methods should be able to deal with real, large-scale cases but [it] is crucial to investigate the role of simplified approaches in providing acceptable solutions’ [15].

To our knowledge, however, there are no prior works that quantify how commercial-scale DG voltage control can impact on relative losses across a wide range of network construction types, levels of demand and permissible voltage rise. This represents a significant gap, as in many systems DG capacity is largely at commercial or utility scale (77% of solar PV capacity is from DGs systems of size >50 kW in the UK [16]). It would be advantageous for such a quantification to build on the simple and practical methods used for calculating Distribution Loss Factors, although ideally the sensitivity and physical causes of the obtained values would also be determined by such a method. We also note the timeliness of this gap, coming as the UK regulator Ofgem implements its Targeted Charging Review, substantially increasing differentiation between customer types via line loss factors [17].

The contribution of this paper is to address this gap by proposing a hybrid approach, combining simulation and analysis to develop an understanding of the proposed Voltage Control Loss Factor (VCLF). This metric attributes losses to voltage control using a Substitution-based approach, and is suitable for evaluation both by simulation (by load flow calculations) or by analysis (in this case using the closed-form solution of a Two-Bus representation of a radial distribution system). This combination of simulation and analysis yields results which are both

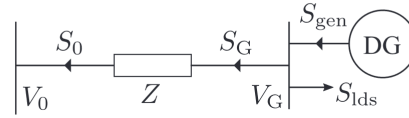


FIGURE 1 The Two-Bus load flow model has a DG and load connected to a sending bus ‘G’, and a receiving, reference bus ‘0’. The load flowing from the sending bus S_G is equal to the sum of the load S_{lds} and DG power S_{gen} . Note that $Z = R + jX$, where R, X denote the resistive and reactive components of the branch, respectively

robust and explainable, enabling utility engineers and decision makers to augment otherwise black-box simulation outputs with sensitivity analysis and physical reasoning.

In Section 2, we describe how reactive power can be used by DGs for voltage control, and introduce the key parameters of the radial Two-Bus model that will be studied in subsequent analysis. In Section 3, we introduce the Voltage Control Loss Factors, to demonstrate how losses can be attributed to a DG using a Substitution-based approach. The value of the VCLF is studied in the context of a fully parameterised Two-Bus model in Section 4, including the analytic calculations of bounds on the value of the VCLF. Case studies demonstrate numerically the robustness of analytic model in Section 5, before conclusions are drawn in Section 6.

2 | VOLTAGE CONTROL FROM DISTRIBUTED GENERATORS AND THE TWO-BUS MODEL

Fine-grained voltage regulation can be achieved using DG voltage control, as this control is based on a continuous PQ capability, in contrast to legacy, discrete control afforded by devices such as Step Voltage Regulators (SVRs). In this section we briefly introduce the principles behind this DG voltage control, and how this operation can lead to substantially increased losses.

If a commercial-scale DG exists on a radial distribution feeder, then generation in excess of the load will flow towards the primary substation, whose voltage is kept close to nominal. Such a configuration is illustrated in Figure 1. The DG and load are connected at the ‘sending’ bus (sending bus quantities are given the subscript $(\cdot)_G$). A ‘receiving’ bus models a primary distribution substation, which sends power to the upstream transmission network (quantities associated with this bus use the subscript $(\cdot)_0$). The voltage at the receiving node $V_0 \in \mathbb{R}$ is the fixed reference voltage, whilst $V_G \in \mathbb{C}$ denotes the voltage at a ‘sending’ node. $S_0, S_G \in \mathbb{C}$ represent the apparent power at the receiving and sending bus, respectively. Finally, the sending node power S_G is equal to the difference of the power of the DG and loads $S_{gen}, S_{lds} \in \mathbb{C}$, that is

$$S_G = S_{gen} - S_{lds}. \quad (1)$$

The ratio of squared voltage magnitudes at the sending and receiving buses of the Two-Bus model can be modelled

according to the approximate ‘LinDistFlow’ equations [18],

$$\frac{|V_G|^2}{|V_0|^2} = 1 + \frac{2(RP_G + XQ_G)}{|V_0|^2}, \quad P_{\text{loss}} = R \frac{P_G^2 + Q_G^2}{|V_0|^2}, \quad (2)$$

where P_{loss} are the line losses, and all other quantities are as previously defined.

The voltage control-losses trade-off can be illustrated by considering (2): to achieve a constant voltage drop as P_G increases (i.e., curtailment is reduced), then Q_G needs to drop at a rate of $P_G R/X$. If some voltage rise is permissible (so that $|V_G|/|V_0|$ is greater than unity), and the reactive load is not capacitive, then losses P_{loss} will increase (as these conditions imply that the magnitude of both P_G and Q_G are increasing (2)). In-turn, these additional losses diminish the primary reason for using the voltage control, which is to reduce curtailment.

This work will consider this trade-off in detail. Fully exploring the solution space requires the use of the non-linear solution of the load flow equation, however [14, 19]. In the sequel, therefore, we will concern ourselves with the exact solution of the Two-Bus model (this will be introduced in Section 4).

2.1 | Remark: Model parameterisation in voltages, impedance and power

Power flow equations, in general, are based on interactions between voltages, impedances and powers (or equivalent derived quantities). These three physical quantities appear in the Two-Bus model as follows:

- the reference voltage V_0 and maximum permissible voltage at the sending bus V_G (voltages);
- the R/X ratio and impedance magnitude $|Z|$ (impedances);
- the demand and generation $S_{\text{ds}}, S_{\text{gen}}$ (powers).

Each of these quantities can vary in time to some degree (e.g., impedance changes through network reconfiguration), although in this work we will only consider temporal changes in demand and generation.

3 | VOLTAGE CONTROL LOSS FACTORS USING SUBSTITUTION

The approach considered in the rest of this work is summarised in Figure 2. It is proposed to evaluate losses attributable to commercial-scale DGs based on a combination of simulation- and analytic-based approaches, with the latter based on a Two-Bus representation. Simulations are used to calculate (in a numerically precise way) losses for a given system in detail. In parallel, the Two-Bus representation is used as a means of understanding the results, considering the physical properties of the network as explanatory factors.

In this section, we outline the Substitution method, which we use to attribute losses to voltage control. We subsequently use

this to define the Voltage Control Loss Factor (VCLF) and the closely related Relative Loss Fraction.

3.1 | Defining voltage control loss factors

The non-linear relationship between power injections and losses means that it is not possible to define a loss allocation algorithm which is not based (to some extent) on some arbitrary policy [20]. Nevertheless, there are many loss allocation algorithms that have been proposed [21–23], and the use of loss allocation by regulators is commonplace.

In this work, we propose to use the method of *Substitution* to calculate loss factors that are appropriate for considering the tradeoff between curtailment, losses and voltage control. This approach has advantages that it is simple to describe and implement, is well-understood by the utility industry, and has been studied for many years in the related problem of loss allocation [24]. For example, Distribution Network Operators (DNOs) in the GB system use this approach to derive line loss factors for DGs [25].

The approach is based on comparing a *Base* case, without some intervention (e.g., a network without DG voltage control) against a counterfactual *Change* case with the intervention enabled. In this work, quantities associated with the Base case are denoted with the superscript $(\cdot)^{\text{base}}$, with quantities associated with the Change case likewise denoted with $(\cdot)^{\text{chng}}$.

The VCLF then compares the change between these two cases in generation and losses, as

$$\text{VCLF} = \frac{\Delta E_{\text{gen}} - \Delta E_{\text{net}}}{\Delta E_{\text{gen}}} \quad (3)$$

$$= \frac{\Delta E_{\text{loss}}}{\Delta E_{\text{gen}}}, \quad (4)$$

where the *net* generation E_{net} is defined as the difference between generation E_{gen} and losses E_{loss} ,

$$E_{\text{net}} = E_{\text{gen}} - E_{\text{loss}}, \quad (5)$$

and the change in energy from the Base to Change case is denoted

$$\Delta E_{(\cdot)} = E_{(\cdot)}^{\text{chng}} - E_{(\cdot)}^{\text{base}}. \quad (6)$$

The VCLF can be positive, zero, negative or undefined. The sign, magnitude and existence of this metric therefore provides quantitative and qualitative information about the impacts of voltage control on losses. If losses are reduced by voltage control, the VCLF will be negative; an increase in losses will give rise to a positive value of the VCLF. Its value is undefined if the operation of a system does not change from the Base to the Change case, as (3) results in the indeterminate form 0/0.

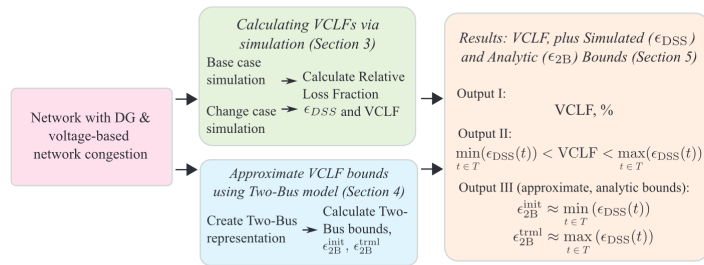


FIGURE 2 This work proposes to study the impact of losses by combining a simulation-based approach with analytic results based on a Two-Bus representation. The outputs of the proposed approach are the Voltage Control Loss Factor (VCLF), VCLF simulation-based bounds based on the relative loss time series ϵ_{DSS} , and (approximate) analytic VCLF bounds based on a Two-Bus representation $\epsilon_{2B}^{\text{init}}, \epsilon_{2B}^{\text{trml}}$.

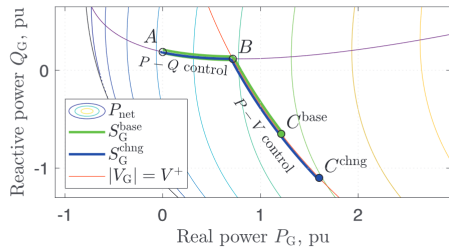


FIGURE 3 An example of a Base and Change case for a system. In this example, a DG is assumed to first minimise losses (with $P-Q$ style control from A to B), before enabling voltage control up to some Base limit (with $P-V$ control from B to C^{base}); the Change limit has increased voltage control capabilities, enables the DG to export fully (at point C^{chng}), albeit with significantly increased reactive flows

3.1.1 | Base and change cases

The Substitution method, in general, can consider arbitrary Base and Change cases to suit a particular system. For example, a Base case may represent a system with no voltage control, with the counterfactual having voltage control enabled. Alternatively, the Base case may have some voltage control allowed up to some reactive power limit, with the Change case using further reactive power.

A simple case is illustrated in Figure 3. Between points A and B , the DG is acting as $P-Q$ generator, minimising the net losses in the system. At the point the upper voltage constraint V^+ is reached, the DG then acts as a $P-V$ generator up to some limit (in the Base case, this is at a real power P_G of 1.2 pu). A DG could upgrade (or request more network capacity) up to the Change case (here at a real power P_G of 1.6 pu); this would lead to reduced curtailment but additional losses (accounted for by the VCLF).

3.2 | The relative loss fraction

The VCLFs are defined over a time period, but in usual circumstances, generation and losses will vary in time t . For example, if

we denote the time-varying generation of the Base and Change as $P_{\text{gen}}^{\text{base}}, P_{\text{gen}}^{\text{chng}}$, respectively, then we can relate generation to Base and Change case respective power limits $\hat{P}_{\text{gen}}^{\text{base}}, \hat{P}_{\text{gen}}^{\text{chng}}$ as

$$P_{\text{gen}}^{\text{base}}(t) \leq \hat{P}_{\text{gen}}^{\text{base}}(t), \quad (7)$$

$$P_{\text{gen}}^{\text{base}}(t) \leq P_{\text{gen}}^{\text{chng}}(t) \leq \hat{P}_{\text{gen}}^{\text{chng}}(t). \quad (8)$$

Note that the time-varying load S_{lds} will (in general) lead to power limits $\hat{P}_{\text{gen}}^{(\cdot)}$ that vary in time.

Naturally, over the course of a year, there will be periods with losses that are identical in the Change and Base cases, and periods when they differ. Therefore, to distinguish between the aggregated VCLF (3) and ‘instantaneous’ values of the VCLF, we define the Relative Loss Fraction ϵ_{DSS} as

$$\epsilon_{DSS}(P_{\text{gen}}^{\text{chng}}, \hat{P}_{\text{gen}}^{\text{base}}) = \frac{\Delta P_{\text{gen}} - \Delta P_{\text{net}}}{\Delta P_{\text{gen}}} \quad (9a)$$

$$= \frac{\Delta P_{\text{ss}}}{\Delta P_{\text{gen}}}, \quad (9b)$$

where the net power generation ΔP_{net} is defined as the difference between the changes in losses ΔP_{ss} and generation ΔP_{gen} (in analogy to (5)), and where the marginal quantities $\Delta P_{(\cdot)}$ are calculated as

$$\Delta P_{(\cdot)} = P_{(\cdot)}^{\text{chng}} - P_{(\cdot)}^{\text{base}}. \quad (10)$$

3.3 | Remark: Bounding VCLFs by consideration relative loss fraction

The main advantages for considering the Relative Loss Fraction ϵ_{DSS} is that the locus of feasible points for that snapshot t can be studied in a more natural way than the VCLF, which is averaged across time. A particularly useful observation is that bounding the Relative Loss Fraction ϵ_{DSS} bounds the VCLF for that loading condition. If all reasonable loading

conditions can be expected to occur during the course of a year, then it is clearly the case for a particular network that

$$\min_{t \in T}(\epsilon_{\text{DSS}}(t)) \leq \text{VCLF} \leq \max_{t \in T}(\epsilon_{\text{DSS}}(t)), \quad (11)$$

where T is the set of all time periods considered. For example, for a system requiring an annual simulation, two load flow calculations would be run for each of $T = \{1, \dots, 8760\}$ for Base and Change cases. The change in losses and generation could then be determined so that $\epsilon_{\text{DSS}}(t)$ could be calculated for each time period using (9b), and then upper and lower bounds computed by determining the maximum and minimum values of these quantities, respectively.

4 | ANALYTIC CHARACTERIZATION USING THE TWO-BUS MODEL

In the previous section, both the VCLF and Relative Loss Fraction ϵ_{DSS} were introduced as a means of considering the losses attributable to voltage control. In this section, we combine that analytic framework with the exact solution of the Two-Bus model to study analytically how the VCLF can vary according to voltage, impedance and power-based parameters introduced in Section 2. We then consider how a distribution network can be modelled using a Two-Bus representation, so analytic predictions can be combined with the simulation-based approach defined in the previous section.

For clarity, we distinguish between the simulation-based Relative Loss Fractions ϵ_{DSS} with values calculated with a Two-Bus representation by denoting the latter with $\epsilon_{2\text{B}}$. The interpretation of these parameters is otherwise identical, although the analytic properties of the latter are (naturally) more straightforward to calculate and study, as we demonstrate in this section.

4.1 | Calculating initial, terminal, and PQ-PV point relative loss fraction

We first consider the minimum and maximum values of $\epsilon_{2\text{B}}$. To begin, note that the Relative Loss Fraction $\epsilon_{2\text{B}}$ is not defined for Change powers equal to than the Base real power constraint $P_{\text{gen}}^{\text{base}}$. However, as this power is approached from above (e.g., as $C^{\text{chng}} \rightarrow C^{\text{base}}$ in Figure 3), the Relative Loss Fraction tends to a constant value we call the *Initial* Relative Loss Fraction, $\epsilon_{2\text{B}}^{\text{init}}$, defined as

$$\epsilon_{2\text{B}}^{\text{init}}(\hat{P}_{\text{gen}}^{\text{base}}) = \lim_{P_{\text{gen}} \rightarrow \hat{P}_{\text{gen}}^{\text{base}}} \epsilon_{2\text{B}}(P_{\text{gen}}, \hat{P}_{\text{gen}}^{\text{base}}) \quad (12)$$

$$= \frac{dP_{\text{loss}}}{dP_{\text{gen}}}(\hat{P}_{\text{gen}}^{\text{base}}). \quad (13)$$

This holds by the definition of the derivative of a function. Similarly, we define a *Terminal* Relative Loss Fraction $\epsilon_{2\text{B}}^{\text{trml}}$ as

$$\epsilon_{2\text{B}}^{\text{trml}}(\hat{P}_{\text{gen}}^{\text{chng}}) = \epsilon_{2\text{B}}(\hat{P}_{\text{gen}}^{\text{chng}}, \hat{P}_{\text{gen}}^{\text{base}}), \quad (14)$$

that is, the value of the Relative Loss Fraction $\epsilon_{2\text{B}}$ in a system when the new, increased power generation limit $\hat{P}_{\text{gen}}^{\text{chng}}$ constrains additional generation.

If a Two-Bus representation provides a good approximation of a given network, the Initial and Terminal Relative Loss Fractions $\epsilon_{2\text{B}}^{\text{init}}, \epsilon_{2\text{B}}^{\text{trml}}$ will approximate the minimum and maximum values of the simulated Relative Loss Fractions,

$$\epsilon_{2\text{B}}^{\text{init}} \approx \min_{t \in T}(\epsilon_{\text{DSS}}(t)), \quad \epsilon_{2\text{B}}^{\text{trml}} \approx \max_{t \in T}(\epsilon_{\text{DSS}}(t)). \quad (15)$$

4.1.1 | The relative loss fraction at the PQ-PV point

For relatively small DG, there will be no need for voltage control, and so the DG can act to minimise losses (between points A and B in Figure 3). The point at which a generator first requires any voltage control we call the *PQ-PV* point, as it occurs when the DG stops behaving like a *P-Q* generator and instead operates as a *P-V* generator. Denoting the sending power at the *PQ-PV* point as $P_{\text{G}}^{\text{PQ-PV}}$, the initial relative loss power with this point as the Base case $\epsilon_{2\text{B}}^{\text{PQ-PV}}$ is found by evaluating (12) with $P_{\text{G}}^{\text{PQ-PV}}$, that is

$$\epsilon_{2\text{B}}^{\text{PQ-PV}} = \epsilon_{2\text{B}}^{\text{init}}(P_{\text{G}}^{\text{PQ-PV}}). \quad (16)$$

For a given load, this point provides a lower bound to $\epsilon_{2\text{B}}^{\text{init}}$, if the DG is operated to minimise losses (so that load reactive power is compensated to minimise losses, as in Figure 3).

4.2 | Analytic solution for relative loss fraction

The voltages and losses of the Two-Bus model can be found as the solution of the implicit equations [14, 19]

$$\left(P_{\text{G}} - \frac{R|V_{\text{G}}|^2}{|Z|^2}\right)^2 + \left(Q_{\text{G}} - \frac{X|V_{\text{G}}|^2}{|Z|^2}\right)^2 = \left(\frac{|V_0||V_{\text{G}}|}{|Z|}\right)^2, \quad (17)$$

$$R_{\text{loss}} = \frac{R}{|Z|} \left(\frac{|V_0|^2 - |V_{\text{G}}|^2}{|Z|} + 2 \frac{P_{\text{G}}R + Q_{\text{G}}X}{|Z|} \right). \quad (18)$$

We now introduce a per-unit system, with powers normalised according to the line short circuit power S_{SC} , impedances against impedance magnitude $|Z|$, and voltages against the reference

voltage $|V_0|$, as

$$s_{(c)} = \frac{S_{(c)}}{S_{SC}}, \quad S_{SC} = \frac{|V_0|^2}{|Z|}, \quad \omega = \frac{|V_G|}{|V_0|}, \quad (19)$$

$$r = \frac{R}{|Z|}, \quad x = \frac{X}{|Z|}. \quad (20)$$

The Two-Bus equations (17), (18) can then be rewritten

$$(p_G - r\omega^2)^2 + (q_G - x\omega^2)^2 = \omega^2, \quad (21)$$

$$P_{ss} = rS_{SC}((1 - \omega^2) + 2(p_G r + q_G x)). \quad (22)$$

Based on these, the terminal Relative Loss Fraction can be calculated as

$$\epsilon_{2B}^{\text{trml}}(P_G^{\text{chng}}, P_G^{\text{base}}) = 2rS_{SC} \left(r + x \frac{\zeta(P_G^{\text{chng}}) - \zeta(P_G^{\text{base}})}{P_G^{\text{chng}} - P_G^{\text{base}}} \right), \quad (23)$$

found by combining (18), (22), and where the mapping from real to reactive powers ζ is (from (21))

$$\zeta(P_G) = x\omega^2 S_{SC} - \sqrt{S_{SC}^2 \omega^2 - (P_G - rS_{SC} \omega^2)^2}. \quad (24)$$

The initial Relative Loss Fraction is given by

$$\epsilon_{2B}^{\text{init}}(P_G^{\text{base}}) = 2r \left(r + x \frac{P_G - r\omega^2 S_{SC}}{\zeta(P_G) - x\omega^2 S_{SC}} \right), \quad (25)$$

where we have used the identity

$$\left. \frac{dQ_G}{dP_G} \right|_{|V_G|} = \frac{P_G - r\omega^2 S_{SC}}{Q_G - x\omega^2 S_{SC}}, \quad (26)$$

as derived from (21).

The PQ - PV initial Relative Loss Fraction ϵ_{2B}^{PQ-PV} (defined in (16)) requires the calculation of P_G^{PQ-PV} . The Appendix shows this power can be found as the solution of a quartic equation.

Finally, for the parameterisation of the full solution space of the Two-Bus model, we also define the generation at the Maximum Power Transfer point, $P_{G, \text{MPT}}$, given by

$$P_{G, \text{MPT}} = S_{SC} \omega (r\omega - (r^2 - x^2)). \quad (27)$$

This can be found by setting the voltage angle at the generator bus to be equal to the impedance angle [14].

4.3 | Characterizing VCLFs in terms of voltage, impedance and power variables using relative loss fractions

We now consider how power, voltage and impedance parameters influence the initial and terminal Relative Loss Fractions

$\epsilon_{2B}^{\text{init}}, \epsilon_{2B}^{\text{trml}}$. Three cases are considered, with the ultimate goal of demonstrating how the value of the VCLF may vary between networks.

4.3.1 | PQ - PV Intersection relative loss fraction

The PQ - PV Relative Loss Fraction ϵ_{2B}^{PQ-PV} is plotted in Figure 4a, as a function of R/X ratio and voltage ratio ω . If the generator compensates the reactive load to minimise losses, this value lower bounds the initial Relative Loss Fraction and is independent of the load.

Clearly visible on this figure is the effect that voltage ratio ω has on ϵ_{2B}^{PQ-PV} , with less of an effect from R/X ratio. Intuitively, this is because the voltage ratio defines the power at which the voltage constraint will become active on the P - Q curve. If the voltage ratio is greater than unity then the voltage constraint will become active when the line is loaded, whilst for the converse the voltage constraint becomes active when the line is still exporting generated power.

Note that there is not always a solution, as the value of P_G^{PQ-PV} does not always exist. This is because loss minimization via reactive power requires a small amount of capacitive reactive power export (see the Appendix, (A.2)), causing the voltage to increase. In these cases, the voltage never drops to the given voltage ratio ω .

4.3.2 | Initial relative loss fraction against uncompensated reactive load

The initial Relative Loss Fraction is plotted as a function of the R/X ratio and the load reactive power q_{lds} in Figure 4b for the case of unity voltage ratio $|V_G| = |V_0|$. Such a condition could occur for the case of uncompensated reactive load (e.g., when a generator exports at unity power factor).

As with ϵ_{2B}^{PQ-PV} , the solution does not exist for some combinations of parameters (due to the discriminant of (24)). If the load is sinking reactive power (positive q_{lds}) then the voltage constraint becomes active at a higher power, increasing the relative losses when voltage control is enabled.

It can be observed from this figure that the reactive load can have a large impact on the initial Relative Loss Fraction. In contrast to the PQ - PV intersection point, the resistance-reactive ratio R/X has a much greater impact, particularly as R/X increases beyond unity.

4.3.3 | Terminal relative loss fraction at maximum power transfer

Finally, the terminal Relative Loss Fraction is calculated at a fraction of the maximum power transfer $P_{G, \text{MPT}}$ in Figure 4c, calculated assuming a voltage ratio ω of unity (and the Base case at no-load). In this case a solution exists at all points, as the maximum power transfer point (27) exists for all R/X . Note that

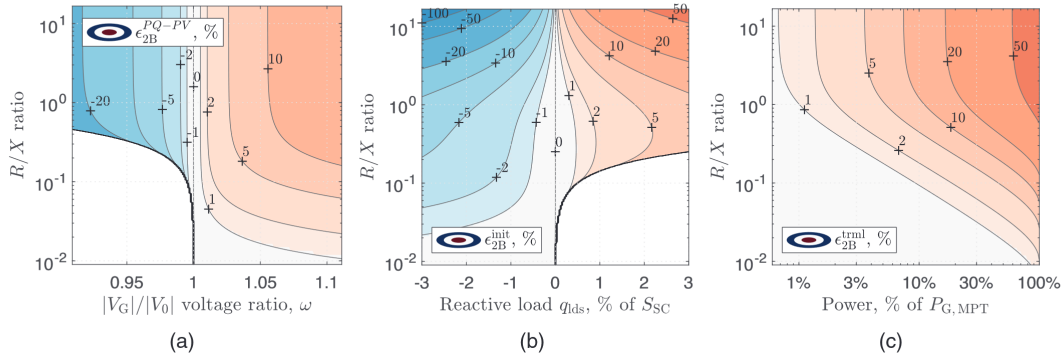


FIGURE 4 Relative power loss fractions for three parameterisations, illustrating how the VCLF metric can vary as a function of impedance, voltage, and power-based parameters. (a) $PQ-PV$ initial Relative Loss Fraction ϵ_{2B}^{PQ-PV} . (b) Initial Relative Loss Fraction ϵ_{2B}^{init} for uncompensated reactive load q_{lds} . (c) Terminal Relative Loss Fraction ϵ_{2B}^{trml} , with the Change case a fraction of the maximum power transfer $P_{G,MPT}$

this characterization does not upper bound the terminal Relative Loss Fraction generally, as the terminal Relative Loss Fraction depends on both the Base and Change points.

It can be observed that the terminal loss fraction can be much higher in cases with high R/X ratios. This can be explained as maximum power transfer at low R/X ratios is associated with steadily decreasing effectiveness of reactive power along circles of constant voltage, whereas maximum power transfer for large R/X ratios are dominated by marginal increases in losses [19].

4.4 | Converting distribution network models to a two-bus representation

In practise, whilst distribution networks are operated radially, individual feeders can still show great variety in their topology. A suitable method is proposed to convert a distribution network to a Two-Bus representation, so that the analytic Two-Bus model can be used to study how the VCLF might vary with different parameters. This approach consists of three main steps, as follows.

- The line impedance Z is calculated as the Thévenin Impedance from the generator to the source (see, e.g., [26, pp. 287-294]).
- The turns ratio of any in-line SVRs are combined to form the overall turns ratio N_{reg} ;
- Finally, the load S_{lds} is found as a linear multiple k_S of the peak load of the circuit $S_{lds, Tot}$,

$$S_{lds} = k_S S_{lds, Tot}. \quad (28)$$

This algorithm will create a Two-Bus representation of the form of Figure 1, with the addition of the turns ratio N_{reg} parameter modifying the voltage ratio ω . It is assumed that this turns ratio

can be considered as an ideal SVR connected directly to the DG, but otherwise the Two-Bus representation of Figure 1 remains unchanged. Note that the calculation of the line impedance (a) from the system admittance matrix can be verified, for example, by perturbing the real and reactive injections at the generator bus and running a load flow to calculate the voltage change, from which the resistance and reactance can be approximated from the LinDistFlow equations (2).

It is proposed that k_S be chosen according to one of the following methods.

- Full load (set $k_S = 1$). The total feeder load is connected to generator node.
- No load ($k_S = 0$). No load is connected at the generator node.
- Weighted load. Load is connected according to the reactive load flowing through the generator bus towards the substation $S_{to sub}$ and the mean demand μ_r (as a % of peak demand $S_{lds, Tot}$) as

$$k_S = \mu_r \frac{|Q_{to sub}|}{|Q_{lds, Tot}|}. \quad (29)$$

The performance of each of these three approaches for calculating k_S is considered in detail in Section 5.3.2, along with a validation of the accuracy of these models for the task in Section 5.3.3.

4.4.1 | Remark: Time-varying models

In the real network cases, the demand varies as a function of time. Rather than determining bounds at all time periods, in (29) we instead opt for a more parsimonious approach, using just one Two-Bus condition to represent a whole year (or other suitable time period of interest). In other words, the approach

we have proposed identifies a set of Two-Bus parameters (Z , S_{ids} , $|V_0|$, $|V_G|$), from which a unique snapshot estimate is obtained for the whole annual time period, calculated using (23), (25) (as highlighted in Figure 2). As we discuss in the next section, this approach results in good numerical performance. Future investigations could consider alternatives, such as time-varying bounds, although we note that this would increase the complexity of the approach.

5 | CASE STUDIES

The framework proposed in this work is now considered, with the simulation-based metrics (Section 3) combined with analytic Two-Bus representations (Section 4) across a range of case studies. Three networks are studied, between them covering multiple voltage levels, a range of R/X ratios, and varying numbers of existing voltage regulation equipment (SVRs).

In this section, the networks and their Two-Bus representations are first described, alongside the temporal profiles assumed for the DG generation and load. To illustrate the close link between VCLF and Relative Loss Fractions, a case study is then considered in detail, clearly demonstrating how voltage control can increase losses, but also demonstrating how the Two-Bus representation augments the understanding of the VCLF. The results of from all three networks are combined to demonstrate the suitability of the approach for understanding the link between network parameters and the VCLF. Finally, the results are then discussed in the context of related prior approaches, highlighting how the approach yields new qualitative results.

5.1 | Case study setup

Three network models are considered in this work, covering a range of voltages levels, permissible voltage drops and R/X ratios. The first two of these networks are IEEE test networks: the EU LV and 34 Bus networks, described in [27]. The former is an urban, European-style low voltage network, whilst the latter is a long, rural US-based feeder, with two in-line SVRs and a substation-based load tap changer (LTC). The third and final network considered is the EPRI K1 feeder. This is also a US-based network [28], although there are no SVRs and the impedance ratio R/X is much lower than the 34 Bus network. This can be seen by considering the two-Bus representative models for these three networks, given in Table 1.

Between the three networks, six case studies are considered, with a range of control types and generator sizes (Table 2). In all cases the DG is assumed to be interfaced such that reactive power can always be generated if required (i.e., ‘VAR priority’, as is mandated by, e.g., the Californian ‘Rule 21’ standard [29]). Changes in voltage control are represented by changes in the reactive power limits of the DG.

The six case studies, labeled from A-F, are designed to consider the following points.

TABLE 1 Calculated Two-Bus properties, with base voltage of 69, 13.2, 0.4 kV and power bases are 2.5, 12, 0.8 MVA for the 34 Bus, EPRI K1 and EU LV circuits, respectively

Circuit(Studies)	Gen. Bus	V_+ , pu	Two-Bus Parameters, pu				
			R/X	$ Z $	$ V_0 $	$ V_G $	$S_{\text{ids, Tot}}$
34 Bus (A, B)	834	1.05	1.85	0.20	1.045	1.056	$0.62 \angle 31^\circ$
34 Bus (C)	834	1.05	1.85	0.20	1.045	1.14	$0.62 \angle 31^\circ$
K1	34096115	1.03	0.26	0.18	1.0	0.99	$0.78 \angle 6.4^\circ$
EU LV	801	1.10	3.34	0.50	1.05	1.053	$0.04 \angle 18^\circ$

- Cases Studies A, D, and E are not permitted to sink reactive power to provide voltage control in the Base case. The R/X ratio of the network changes significantly between these cases.
- The amount of reactive power that can be used for voltage control increases from Study A to Study B, and from Study E to Study F.
- Voltage controls from voltage regulators change from Study A to Study C, with fixed reactive power constraints for the DG.

All case studies assume that the DG is operated to minimise net demand (i.e., minimise losses and curtailment), a very common objective in distribution network operation [30]. To calculate the reactive powers to achieve this goal, the Golden Search method was used to minimise losses (when networks voltages are below their upper limit), and the secant method was used to find the reactive power required for $P-V$ control (these algorithms are described in [31, Ch. 4]).

5.1.1 | Load and generation data

A representative load profile for each of the loads in the 34 Bus and EPRI K1 circuits was obtained by averaging and normalizing 23 smart meter profiles from [32]. Individual profiles were used for each load in the EU LV network. All loads were scaled to 78% of their nominal kVA ratings for the 34 Bus so that the load flow is feasible. A solar profile was obtained using typical meteorological year (TMY) data [33] for London Gatwick. These were then used to determine the load weighting coefficient k_S (29).

5.1.2 | Existing voltage control devices

For the case studies with the 34 Bus circuit (A, B, C), voltage regulator line drop compensation (LDC) settings were modified according to Table 3, to avoid undervoltages on branches coming off the main feeder. For Study A and Study B the substation (source) voltage was reduced by 0.5% and the fixed tap ratio on the substation transformer ‘xfm1’ was increased by one tap. For Study C, the substation was additionally assumed to have a load tap changer (LTC) installed, with LDC enabled. Additionally,

TABLE 2 Generator sizing and reactive power (Q) constraints for each case study. Generator apparent power export is constrained to be less than the generator inverter rating S_+

ID (ckt.)	Gen. power rating, kW	Gen. inverter rating S_+ , kVA	Base Q , Q_-^{base} , kVAr	Chng. Q , Q_-^{chng} , kVAr	Load weighting k_S , (29)
A (34 Bus)	1250	1400	0	400	0.31
B (34 Bus)	1250	1400	400	800	0.31
C (34 Bus)	3000	3200	0	400	0.31
D (K1)	15,000	16,000	0	750	0.04
E (EU LV)	55	68	0	20	0.004
F (EU LV)	55	68	20	40	0.004

TABLE 3 Line Drop Compensation (LDC) and tap limits for the SVRs and LTC in the 34 Bus circuit

SVR ID	LDC parameters, V				Min tap	
	R_{reg}	X_{reg}	V_{reg}	Max tap	Studies A, B	Study C
Reg. 1	4	1.6	118	+16	−1	−6
Reg. 2	0.8	0.8	124	+16	−2	−16
LTC	15	6	120	+2	NA	−6

the capacitors at the end of the feeder were switched out, as the generator (located close to these capacitors) was available to provide compensation more precisely.

5.2 | Case study example: IEEE 34 bus, study A

The generator power for Study A on two illustrative days is shown in Figure 5a,c, and the corresponding voltages from the network are plotted in Figure 5b,d. The voltages remain in bounds across the whole network in both Base and Change cases. There is an increase in generation on these two days of 2.72 MWh, and an increase in losses of 0.36 MWh, so the VCLF is 13.2%. Note that the maximum and minimum voltages on the network do not change from the Base to the Change case in Figure 5b,d as the voltage control holds the upper voltage at the upper voltage limit.

The corresponding Relative Loss Fraction ϵ_{DSS} is plotted in Figure 6. At the times when the reactive power of the Change case drops below the reactive power of the Base case, there is a difference in the generation and losses in the network. For times when the powers in both circuits are identical, the Relative Loss Fraction is undefined (and so not plotted on Figure 6).

Additionally, Figure 6 has three pairs of dashed lines plotted, calculated using the Two-Bus representation of the network. The three lines assume either that all load is co-located with the generator ($k_S = 1$), that none of the load is co-located with the generator ($k_S = 0$), or that 31% of the load is co-located ($k_S = 0.31$, from (29)). Each of these bounds are the initial and terminal values of the Relative Loss Fraction, calculated from (23), (25).

TABLE 4 Generation, losses, and corresponding Voltage Control Loss Factor (VCLF, from (3)) for each case study

ID (Ckt.)	Potential Gen., MWh	Gen., MWh		Loss, MWh		VCLF
		Base	Chng.	Base	Chng.	
A (34 Bus)	1414.9	1308.8	1397.8	237.0	248.5	13.0%
B (34 Bus)	1414.9	1397.8	1414.9	248.5	252.1	21.4%
C (34 Bus)	3395.9	3274.2	3359.5	346.0	371.6	30.0%
D (K1)	16, 979	14, 786	16, 979	1550	1602	2.4%
E (EU LV)	62.26	32.04	43.01	0.46	0.95	4.5%
F (EU LV)	62.26	43.01	50.94	0.95	1.83	11.1%

Figure 6 demonstrates two things. First, the Relative Loss Fraction ϵ_{DSS} values are close to the calculated VCLF of 13.2%. Second, the predicted bounds with the Two-Bus weighted load representation $\epsilon_{2B}^{\text{init}}$, $\epsilon_{2B}^{\text{trml}}$ (the pair of blue dashed lines) give reasonably accurate bounds on the Relative Loss Fraction values, illustrating that this network is behaving in a very similar manner to the Two-Bus representation. The full-load ($k_S = 1$) and no-load ($k_S = 0$) bounds show a very large potential change in Relative Loss Fraction with ϵ_{2B} .

5.3 | Results of case studies

The results of all of case studies are now considered, to study how the R/X ratio and voltage rise impact on the VCLF. We also consider how the analytic Two-Bus calculations can provide explanatory factors to distinguish between the varied results of the simulation-based VCLF.

5.3.1 | VCLFs for all cases (A–F) from an annual time series simulation

Table 4 summarises the results of the time series simulation of the six case studies, with the duration of the simulations being one calendar year.

Comparing Studies A and B and Studies E and F, it can be observed that the VCLF increases by more than 6%.

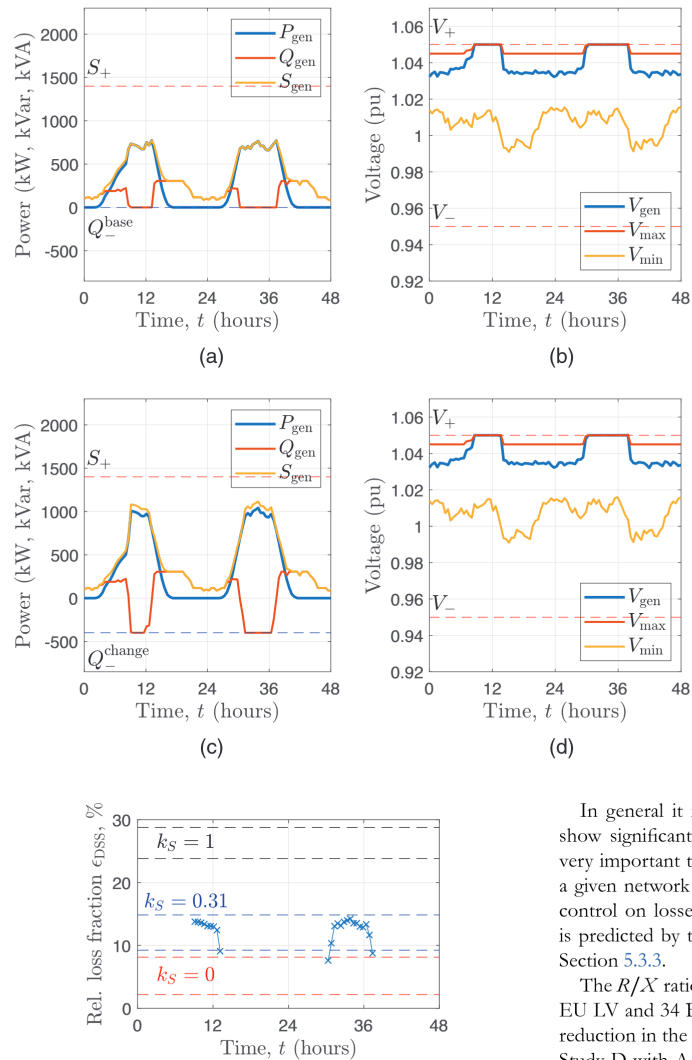


FIGURE 6 Relative Loss Fraction ϵ_{DSS} for two days considered in Study A (powers and voltages as in Figure 5). This leads to an increase in losses; plotting the Relative Loss Fraction ϵ_{DSS} illustrates that this reduces the efficacy of reactive power by 8–14%

Interestingly, however, this increase is less than the increases between Study A and Study C, for which the VCLF increases by 17%. This is driven by the increase in the voltage drop along the line that can occur due to the control from the substation LTC. This highlights clearly how the change in permissible voltage drop, enabled by the drop in substation voltage by the LTC, results in higher currents at the point voltage control is needed, and therefore higher relative losses).

FIGURE 5 Powers (left) voltages (right) and for Study A, with V_{\min} , V_{\max} denoting the minimum and maximum nodal voltages across the network respectively. The Base case [(a) and (b)] has a reactive power limit $Q_{\text{base}}^{\text{base}} = 0$ kVar, whilst the Change case [(c) and (d)] has the limit $Q_{\text{change}}^{\text{base}} = -400$ kVar. Reactive power control increases the amount of power that can be exported by (a) and (c) without the the voltage going beyond bounds V_+ (b) and (d), albeit with increased reactive power flows (a) and (c) and therefore losses. (a) Base Case Powers. (b) Base Case Voltages. (c) Change Case Powers. (d) Change Case Voltages

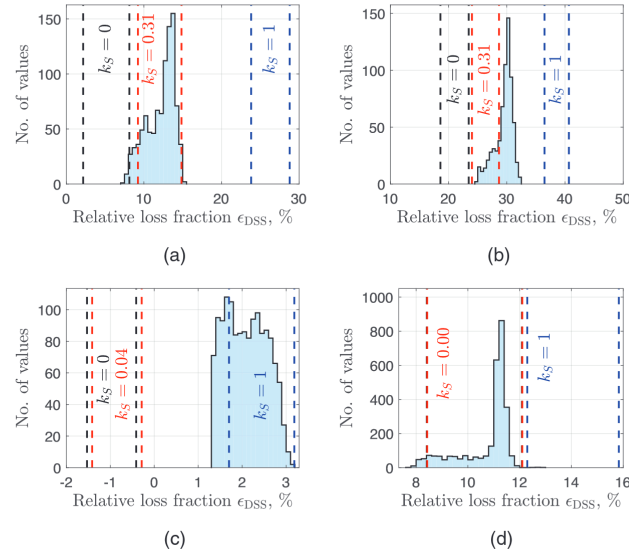
In general it is interesting to see that Studies A, B and C show significant variation in VCLF. This highlights that it is very important to consider the configuration and operation of a given network accurately to calculate the impacts of voltage control on losses. It is important to note that this behaviour is predicted by the Two-Bus representations, as considered in Section 5.3.3.

The R/X ratio of the EPRI K1 circuit is much lower than the EU LV and 34 Bus circuit. There is therefore a corresponding reduction in the VCLF for this circuit (for example, comparing Study D with A and E). However, as pointed out, the EU LV circuit has a lower Relative Loss Fraction than the 34 Bus circuit, even though the R/X ratio of the EU LV circuit is higher. As predicted by the Two-Bus representation, the R/X ratio is just one factor, with other parameters (the load reactive power Q_{lds} and voltage ratio $\omega = |V_G|/|V_0|$) also making a substantial contribution to the calculated value.

5.3.2 | Histograms of relative loss fraction

Histograms of the Relative Loss Fraction ϵ_{DSS} from each half hour period are plotted in Figure 7 for four of the case studies alongside the bounds predicted by the Two-Bus representation ϵ_{2B} . Note that for Case Study F, the Weighted load multiplier k_S

FIGURE 7 Histogram of the Relative Loss Fraction values for Studies A, C, D and F. The three sets of dashed vertical lines correspond to calculated Relative Loss Fractions ϵ_{2B}^{init} , ϵ_{2B}^{trml} calculated at three load weightings (as described in Section 5.2). Comparing (a)–(d), it can be observed that the Two-Bus representations ϵ_{2B}^{init} , ϵ_{2B}^{trml} are successful at identifying the magnitude and spread of the Relative Loss Fractions ϵ_{DSS} . (a) Study A (34 Bus). (b) Study C (34 Bus). (c) Study D (EPRI K1). (d) Study F (EU LV)



(from (29)) is very close to zero, and so for clarity the no-load weighting ($k_S = 0$) is not plotted on this figure.

There are three things that can be noted from Figure 7. First, it is clear that there are non-trivial lower bounds on the Relative Loss Fraction ϵ_{DSS} . Comparing these figures with the VCLF from Table 4, it can be observed that the VCLF is always within 6% of the maximum and minimum Relative Loss Fraction.

Second, the range of the values of the Relative Loss Fraction ϵ_{DSS} are increased somewhat compared to the Two-Bus model (i.e., the difference between the maximum and minimum values of ϵ_{DSS} is greater than the difference between ϵ_{2B}^{init} , ϵ_{2B}^{trml}). This is not unexpected, as the Two Bus representations here only considers a single loading point.

Finally, we note that the between-network predictions prove to be remarkably accurate; this indicates that the Two-Bus model appears to be providing very good physical explanations for the differences observed in the VCLF. The EPRI K1 circuit has the weakest estimate in relative terms; it is thought that this is because there is a bulk capacitor upstream of the DG, leading to a different reactive power profile to the other feeders (which only have inductive loads).

5.3.3 | Relative loss fraction bounds

To summarise the results of this section, the minimum and maximum values of the simulated Relative Loss Fractions ϵ_{DSS} are compared against the bounds calculated using the Two-Bus representation ϵ_{2B} with the ‘weighted’ load method (the red dashed lines of Figure 7). These values are tabulated in Table 5.

It can be seen that there is no more than 5% difference between the maximum value of ϵ_{DSS} and the equivalent

TABLE 5 Simulation-based (OpenDSS) and Analytic-based (Two-Bus) VCLF bounds for each of the six case studies. Simulation bounds are determined as in (11), whilst analytic (Two-Bus) bounds are determined using (23) and (25)

Study	Circuit	Simulation (OpenDSS), %		Analytic (Two-Bus), %	
		$\min(\epsilon_{DSS})$	$\max(\epsilon_{DSS})$	ϵ_{2B}^{init}	ϵ_{2B}^{trml}
A	34 Bus	7.5	15.2	9.2	14.8
B	34 Bus	18.1	23.0	20.1	25.3
C	34 Bus	24.6	32.3	24.0	28.7
D	EPRI K1	1.3	3.1	−1.4	−0.3
E	EU LV	0.8	5.4	0.7	4.6
F	EU LV	7.8	12.9	8.4	12.1

Two-Bus values ϵ_{2B}^{trml} ; similarly, there is no more than a 4% difference between the minimum value of ϵ_{DSS} and initial Relative Loss Fraction ϵ_{2B}^{init} . It is concluded that the Two-Bus representation predicts the between-case behaviour of each network with very good accuracy.

5.4 | Discussion—Comparison with related approaches and promising research directions

The combination of the analytic (Two-Bus) approach with detailed simulations shows similarities with [10–12]. The authors of [12] highlight reasons as to why certain DG generation profiles lead to a greater curvature in the total losses with DG penetration (i.e., a narrower ‘U-shaped curve’), whilst the authors of [10] present analytic arguments to propose improved settings for inverter controls. In a similar way, this

paper determines new qualitative results which are supported by a range of detailed simulations. For example, we have shown that network voltage drop has a huge effect on relative losses when using voltage control, and we have also clearly demonstrated the existence of non-trivial bounds on the VCLF. To our knowledge, these points have not been explored in prior works, with the exception of related analytic results we first presented in [11] for the related (but distinct) valuation error metric. Here we present a wider range of analysis (e.g., considering PQ and PV control), and provide detailed simulations that were missing in that earlier paper—the simulations in this work have enabled the validation of the approach comprehensively.

It is interesting to note that some prior works that consider changes in losses and curtailment present only the changes calculated as a fraction of peak demand, rather than the change in losses with respect to changes in curtailment (i.e., some works only $\Delta E_{\text{loss}}/E_{\text{loss}}^{\text{base}}$, instead of the VCLF (3)) [6, 34]. By considering Table 4, it can be seen that this fractional change in losses is not necessarily informative—the relative increase in losses with respect to changes in curtailment is typically much greater than with respect to system demand (e.g., the system losses only increase 7% in Study C, where the VCLF has a value of 30%). The VCLF metric (or other relative measures of losses with respect to curtailment) are therefore strongly preferred in the evaluation of DG reactive power control.

In this work, we have focussed on studying the whole Two-Bus solution space (right up to maximum power transfer) alongside a number of detailed simulations. Future work could look to constrain the solution space of the Two-Bus analysis, considering the applicable service area of particular DNOs and voltage levels considering their unique operational and design procedures (which vary significantly). The explainability and robustness of analytic approaches such as that presented in this work would allow engineers identifying potential approaches to improve their practise with respect to metrics such as VCLF. Future work could also consider more sophisticated approaches for developing Two-Bus network representations, alternative DG control approaches (such as droop control), or the explicit development of suitable incentives to encourage voltage control in a responsible and appropriate way.

6 | CONCLUSIONS

This paper considers how voltage control by DGs can impact on distribution losses, given that sinking reactive power typically increases losses, diminishing the effectiveness of this control. Radially operated DGs are studied using a combination of simulation and analytic approaches, using the Voltage Control Loss Factor and Two-Bus representation of a network to understand how these losses can vary with R/X ratio, permissible voltage rise and network load.

The impact of permissible voltage rise is shown to be particularly striking, but previous works have often neglected to consider this aspect in sensitivity analysis. This point is particularly important to note as the permissible voltage rise varies between

systems at the same voltage levels (due to differing voltage set-points at substations) and between voltage levels (due to different regulatory requirements at LV, MV and HV distribution). Distribution systems with different construction and operating settings could therefore see highly heterogeneous performance of voltage control with respect to losses.

The combination of reduced reactive power-voltage sensitivity and increased losses makes reactive power control significantly less attractive in systems with R/X ratios greater than unity. This observation is corroborated by a yearly time-series analysis of three DGs in three unbalanced distribution network models, with as much as 30% of additional generation transferred directly as line losses. This result is explained succinctly with an analytic Two-Bus representation of the network, with bounds on the relative losses predicted to within 5% across six case studies.

The use of voltage control in distribution networks is set to become an integral part of DSO planning and operations, both from commercial-scale DG systems providing active network management, and by the widespread use of rule-based droop control by domestic-scale DGs. We conclude by noting that the results of this work illustrate that equitable future loss allocation algorithms will require very careful design in systems with DG voltage control, with widely varying R/X ratios, demands and substation set points all having a significant impact on additional losses. Being able to explain clear reasons for variable loss factors across the network could result in more sophisticated and equitable loss allocation mechanisms becoming acceptable, ultimately enabling suitable price signals to incentivise prosumer investment in appropriate smart grid technologies.

ACKNOWLEDGEMENTS

The authors gratefully acknowledge the Oxford Martin Programme on Integrating Renewable Energy, the Clarendon Scholarship and the John Aird scholarship for supporting this work.

CONFLICT OF INTEREST

The authors have declared no conflict of interest.

NOMENCLATURE

R	Resistance, Ω / pu
X	Reactance, Ω / pu
Z	Complex impedance, Ω / pu
$P_{(i)}$	Active power, kW / pu
$Q_{(i)}$	Reactive power, kVAr / pu
$S_{(i)}$	Complex power, kVA / pu
$V_{(i)}$	Complex voltage, kV / pu
$E_{(i)}$	Energy, kWh
t	Time index, hours
T	Set of all considered time periods
VCLF	Voltage Control Loss Factor (in energy)
$\epsilon_{(i)}$	Relative Loss Fraction (in power)
S_{SC}	Line short circuit power, MVA
$s_{(i)}$	Normalised power $S_{(i)}/S_{\text{SC}}$
ω	Voltage magnitude ratio $ V_G / V_0 $
r	Resistance fraction $R/ Z $

X	Reactance fraction $X/ Z $
ζ	Function mapping real powers to reactive powers on voltage level sets
N_{reg}	Overall turns ratio of voltage regulators
k_S	Fraction of the total demand allocated to the generator node in the Two-Bus network representation, %
$S_{\text{ds,Tot}}$	Total demand of a distribution network, kVA
Q_{tsub}	Reactive load flowing to the substation from the generator node, kVAr
μ_t	Mean demand as a fraction of peak demand $S_{\text{ds,Tot}}$, %
$(\cdot)_+, (\cdot)_-$	Limits on a variable—maximum and minimum respectively
$(\cdot)_G$	Variable associated with the ‘sending’ (DG) node
$(\cdot)_0$	Variable associated with the ‘receiving’ (substation) node
$(\cdot)_{\text{lds}}$	Variable associated with a load
$(\cdot)_{\text{gen}}$	Variable associated with the generator
$(\cdot)_{\text{net}}$	Variable associated with net power (generation less losses)
$(\cdot)_{\text{iss}}$	Loss-based variable (energy or power)
$(\cdot)_{\text{base}}$	Variable associated with the Base case (no DG reactive power control)
$(\cdot)_{\text{chng}}$	Variable associated with the Change case (with DG reactive power control)
$(\cdot)_{2B}$	Variable associated with non-linear Two-Bus network solution
$(\cdot)_{\text{DSS}}$	Variable associated with an iterative power flow solution (distribution system simulator)
$(\cdot)_{G,\text{MPT}}$	Variable associated with the maximum power transfer point of a generator
$\hat{(\cdot)}$	Maximum generator power export limit
$(\cdot)_{\text{init}}$	Variable associated with the ‘Initial’ DG generation point (max DG export in Base case)
$(\cdot)_{\text{trml}}$	Variable associated with the ‘Terminal’ DG generation point (max DG export in Change case)
$(\cdot)^{PQ-PV}$	Variable associated with the point at which PQ DG operation (loss minimization) is replaced with PV optimization (voltage control)
$(\cdot)_{\text{reg}}$	Voltage regulator Line Drop Compensation parameters, V
$ \cdot $	Absolute value of a quantity

ORCID

Matthew Deakin  <https://orcid.org/0000-0002-1291-1317>

Dimitra Apostolopoulou  <https://orcid.org/0000-0002-9012-9910>

REFERENCES

- Turitsyn, K., Šulc, P., Backhaus, S., Chertkov, M.: Options for control of reactive power by distributed photovoltaic generators. *Proc. IEEE* 99(6), 1063–1073 (2011)
- Nikolaïdis, A.I., Charalambous, C.A.: Hidden cross-subsidies of net energy metering practice: energy distribution losses reallocation due to prosumers’ and storsumers’ integration. *IET Gener. Transm. Distrib.* 11(9), 2204–2211 (2017)
- Elexon Ltd.: Production, submission, audit and approval of line loss factors. <https://www.elexon.co.uk/documents/bsc-codes/bscps/bscp128-3/>, 2020. Accessed April 2021
- Anastasiadis, A.G., Argyropoulou, V.M., Pagonis, K.D., Hatzigiorgiou, N.D.: Losses in a LV-microgrid with the presence of reactive power and CHP units. In: 8th Mediterranean Conference on Power Generation, Transmission, Distribution and Energy Conversion. IEEE, Piscataway (2012)
- Gil, H.A., Joos, G.: Models for quantifying the economic benefits of distributed generation. *IEEE Trans. Power Syst.* 23(2), 327–335 (2008)
- O’Connell, A., Keane, A.: Volt-var curves for photovoltaic inverters in distribution systems. *IET Gener. Transm. Distrib.* 11(3), 730–739 (2017)
- Chen, X., Yi, Y., Zhang, Y., Li, Q., Zhu, J., Cai, Z.: Approach to setting gateway reactive power control band for distribution networks with wind power. *IET Gener. Transm. Distrib.* 11(3), 596–604 (2017)
- Kouveliotis-Lysikatos, I., Hatzigiorgiou, N.: Fully distributed economic dispatch of distributed generators in active distribution networks considering losses. *IET Gener. Transm. Distrib.* 11(3), 627–636 (2017)
- Zhou, Q., Bialek, J.: Generation curtailment to manage voltage constraints in distribution networks. *IET Gener. Transm. Distrib.* 1(3), 492–498 (2007)
- Bletterie, B., Kadam, S., Bolgarny, R., Zegers, A.: Voltage control with PV inverters in low voltage networks in depth analysis of different concepts and parameterization criteria. *IEEE Trans. Power Syst.* 32(1), 177–185 (2016)
- Deakin, M., Morstyn, T., Apostolopoulou, D., McCulloch, M.: The value of reactive power for voltage control in lossy networks. In: 2018 IEEE Power & Energy Society General Meeting (PESGM), pp. 1–5. IEEE, Piscataway (2018)
- Quezada, V.M., Abbad, J.R., Roman, T.G.S.: Assessment of energy distribution losses for increasing penetration of distributed generation. *IEEE Trans. Power Syst.* 21(2), 533–540 (2006)
- Zecchino, A., Marinelli, M.: Analytical assessment of voltage support via reactive power from new electric vehicles supply equipment in radial distribution grids with voltage-dependent loads. *Int. J. Electr. Power Energy Syst.* 97, 17–27 (2018)
- Vournas, C.: Maximum power transfer in the presence of network resistance. *IEEE Trans. Power Syst.* 30(5), 2826–2827 (2015)
- Abbey, C., Baïtch, A., Bak-Jensen, B., Carter, C., Celli, G., El Bakari, K., Fan, M., Georgilakis, P., Hearne, T., Ochoa, L.N.: Planning and Optimization Methods for Active Distribution Systems. CIGRE, Paris (2014)
- Department of Energy and Climate Change: National statistics: Solar photovoltaics deployment in the UK. <https://www.gov.uk/government/statistics/solar-photovoltaics-deployment>. Accessed April 2021
- Office for Gas and Electricity Markets (OFGEM): Targeted charging review: Decision and impact assessment (2019)
- Baran, M.E., Wu, F.F.: Optimal capacitor placement on radial distribution systems. *IEEE Trans. Power Delivery* 4(1), 725–734 (1989)
- Deakin, M., Morstyn, T., Apostolopoulou, D., McCulloch, M.: Loss induced maximum power transfer in distribution networks. In: 2018 Power Systems Computation Conference (PSCC), pp. 1–7. IEEE, Piscataway (2018)
- Exposito, A.G., Santos, J.R., Garcia, T.G., Velasco, E.R.: Fair allocation of transmission power losses. *IEEE Trans. Power Syst.* 15(1), 184–188 (2000)
- Mutale, J., Strbac, G., Curcic, S., Jenkins, N.: Allocation of losses in distribution systems with embedded generation. *IEE Proc. Gener. Transm. Distrib.* 147(1), 7–14, (2000)
- Conejo, A., Arroyo, J., Alguacil, N., Guijarro, A.: Transmission loss allocation: a comparison of different practical algorithms. *IEEE Trans. Power Syst.* 17(3), 571–576 (2002)
- Yu, Q., Xie, J., Chen, X., Yu, K., Gan, L., Chen, L.: Loss allocation for radial distribution networks including DGs using Shapley value sampling estimation. *IET Gener. Transm. Distrib.* 13(8), 1382–1390 (2019)
- Costa, P.M., Matos, M.A.: Loss allocation in distribution networks with embedded generation. *IEEE Trans. Power Syst.* 19(1), 384–389 (2004)
- Elexon: LDSO methodology statements. www.elexonportal.co.uk/ldsomethodologystatements, 2021, accessed April (2021)
- Grainger, J.J., Stevenson Jr., W.D.: Power System Analysis. McGraw-Hill, New York (1994)

27. Schneider, K.P., Mather, B., Pal, B., Ten, C.-W., Shirek, G.J., Zhu, H., Fuller, J.C., Pereira, J.L.R., Ochoa, L.F., de Araujo, L.R., et al.: Analytic considerations and design basis for the IEEE distribution test feeders. *IEEE Trans. Power Syst.* 33(3), 3181–3188 (2017)
28. Electric Power Research Institute (EPRI): Hosting capacity feeders J1, K1, M1. https://dpv.epri.com/feeder_models.html. Accessed 19 April 2019
29. Pacific Gas and Electricity Company: Electric rule no. 21: Generating facility interconnections. https://www.pge.com/tariffs/tm2/pdf/ELEC_RULES_21.pdf. Accessed 9 Sept 2019.
30. Antoniadou-Plytaria, K.E., Kouveliotis-Lysikatos, I.N., Georgilakis, P.S., Hatziaargyriou, N.D.: Distributed and decentralized voltage control of smart distribution networks: models, methods, and future research. *IEEE Trans. Smart Grid* 8(6), 2999–3008 (2017)
31. Gill, P.E., Murray, W., Wright, M.H.: *Practical Optimization*. Academic Press, London (1981)
32. Engineering, I.B.: Energy demand research project: Early smart meter trials, 2007–2010. UK Data Service
33. Dobos, A.P.: PVWatts version 5 manual. Technical Report. National Renewable Energy Lab. (NREL), Golden (2014)
34. Ochoa, L.F., Dent, C.J., Harrison, G.P.: Distribution network capacity assessment: Variable DG and active networks. *IEEE Trans. Power Syst.* 25(1), 87–95 (2010)

How to cite this article: Deakin, M., Morstyn, T., Apostolopoulou, D., McCulloch, M. D.: Voltage control loss factors for quantifying DG reactive power control impacts on losses and curtailment. *IET Gener. Transm. Distrib.* 16, 2049–2062 (2022).
<https://doi.org/10.1049/gtd2.12413>

APPENDIX: THE PQ – PV POINT AS THE SOLUTION OF A FOURTH ORDER POLYNOMIAL (QUARTIC EQUATION)

Here we briefly demonstrate how the PQ – PV intersection point (defined in Section 4.1.1) can be found numerically as the solution of a quartic equation. First, differentiating the losses for fixed P_G (from (21), (22)), setting to zero and rearranging yields

$$\frac{R}{X} Q_G^2 - \left(2P_G + \frac{V_0^2}{R} \right) Q_G + \frac{X}{R} P_G^2 = 0. \quad (\text{A.1})$$

The optimal root is the smaller of the two roots, is denoted by Q_G^L , and is given by

$$Q_G^L(P_G) = \frac{X}{R} \left((P_G + q_p) - \sqrt{(P_G + q_p)^2 - P_G^2} \right), \quad (\text{A.2})$$

where $q_p = V_0^2/2R$. Setting $Q_G^L(P_G) = \zeta(P_G)$ (from (24)) yields an expression of the form $\alpha(P_G) + \sqrt{\beta(P_G)} = \sqrt{\gamma(P_G)}$ where α is a polynomial of order 1, and β, γ are of order 2. This is therefore rationalised as a quartic polynomial

$$\alpha^2(\alpha^2 - 2(\beta + \gamma)) + \beta^2 + \gamma^2 - 2\beta\gamma = 0. \quad (\text{A.3})$$